

Small Molecule Inhibitors of Dynamin I GTPase Activity: Development of Dimeric Tyrphostins

Timothy Hill,[†] Luke R. Odell,[†] Jennifer K. Edwards,[†] Mark E. Graham,[‡] Andrew B. McGeachie,[‡] Jenny Rusak,[‡] Annie Quan,[‡] Ruben Abagyan,[§] Janet L. Scott,^{||} Phillip J. Robinson,^{*,‡} and Adam McCluskey^{*,†}

Discipline of Chemistry, Chemistry Building, School of Environmental and Life Sciences, The University of Newcastle, Callaghan, NSW 2308, Australia, Children's Medical Research Institute, 214 Hawkesbury Road, Westmead NSW 2145, Australia, Department of Molecular Biology, The Scripps Research Institute, 10550 North Torrey Pines Road, TCP-28, La Jolla, California 92037, and Centre for Green Chemistry, PO Box 23, Monash University, Victoria 3800, Australia

Received December 1, 2004

Dynamin I is a GTPase enzyme required for endocytosis and is an excellent target for the design of potential endocytosis inhibitors. Screening of a library of tyrphostins, in our laboratory, against the GTPase activity of dynamin I gave rise to a μM potent lead, 2-cyano-3-(3,4-dihydroxyphenyl)thioacrylamide (**1**, IC_{50} 70 μM). Our initial investigations suggested that only the dimeric form of **1** displayed dynamin I GTPase inhibitory activity. Subsequent synthetic iterations were based on dimeric analogues and afforded a number of small molecules, low μM potent, inhibitors of dynamin I GTPase, in particular, symmetrical analogues with a minimum of two free phenolic $-\text{OH}$ s: catechol-acrylamide (**9**) (IC_{50} = $5.1 \pm 0.6 \mu\text{M}$), its 3,4,5-trihydroxy congener (**10**) (IC_{50} = $1.7 \pm 0.2 \mu\text{M}$), and the corresponding 3-methyl ether (**11**) (IC_{50} = $9 \pm 3 \mu\text{M}$). Increasing the length of the central alkyl spacer from ethyl to propyl (**22–24**) afforded essentially identical activity with IC_{50} 's of 1.7 ± 0.2 , 1.7 ± 0.2 , and $5 \pm 1 \mu\text{M}$, respectively. No decrease in activity was noted until the introduction of a hexyl spacer. Our studies highlight the requirement for two free amido NHs with neither the mono-*N*-methyl (**86**) nor the bis-*N*-methyl (**87**) analogues inhibiting dynamin I GTPase. A similar effect was noted for the removal of the nitrile moieties. However, modest potency was observed with the corresponding ester analogues of **9–11**: ethyl ester (**90**), propyl ester (**91**), and butyl ester (**92**), with IC_{50} 's of 42 ± 3 , 38 ± 2 , and $61 \pm 2 \mu\text{M}$, respectively. Our studies reveal the most potent and promising dynamin I GTPase inhibitor in this series as (**22**), which is also known as BisT.

Introduction

Mammalian cells take up extracellular material and recycle their membranes by endocytosis, which is the formation of numerous types of membrane vesicles at the plasma membrane.^{1–3} Vesicles occur in different sizes, ranging from large phagosomes, smaller clathrin-coated vesicles to tiny synaptic vesicles (SV). Endocytic mechanisms subserve many cellular functions including the uptake of extracellular nutrients, regulation of cell-surface receptor expression and signaling, antigen presentation, and maintenance of synaptic transmission. Among the various endocytic pathways are two that are biochemically well-characterized. The first is the rapid *synaptic vesicle endocytosis* (SVE) that follows vesicle exocytosis in nerve terminals. SVE is not specifically linked to receptor activation, but serves to retrieve empty SVs for later refilling.^{2,3} It requires the enzyme dynamin I.^{4,5} The second is *receptor-mediated endocytosis* (RME) which is initiated upon ligand binding to cell surface receptors and occurs via clathrin-coated pits in all cells, including nerve terminals. It requires dynamin II.⁴ RME provides the main entry point into cells for plasma membrane components (such as the receptor–ligand complexes and membrane lipids) or for extracellular fluid.

Multiple endocytosis inhibitors exist, e.g., chlorpromazine,⁶ concanavalin A, phenylarsine oxide,⁷ dansyl-

cadaverine,⁸ intracellular potassium depletion,⁹ intracellular acidification,¹⁰ and decreasing medium temperature to 4 °C.⁶ Each of these methods has poor specificity and limited utility and no specific biological target. Nonetheless, their use has contributed to a better understanding of endocytosis. Some have been used to demonstrate that blocking endocytosis might eventually have clinical applications for humans.¹¹

Targeting the GTPase activity of dynamin is a more attractive candidate for an endocytosis inhibitor than any currently known targets. There are three dynamin genes, with dynamin I in neurons, dynamin II being ubiquitously expressed and dynamin III in neurons and testes.^{4,5} All dynamins have four main domains which are potential drug targets. (i) The GTPase domain has an unusually low affinity for GTP (10–25 μM) and extremely high turnover rates compared with other GTPases. It is required for vesicle fission.^{4,12} The crystal structure of this domain of dynamin from *Dictyostelium* was recently solved.¹³ (ii) The pleckstrin homology (PH) domain is both a targeting domain and potentially a GTPase inhibitory module and is essential for endocytosis.⁵ Dynamin interacts with lipids via this domain, and dynamin binding to nanotubules containing phosphatidylinositol bisphosphate ($\text{PtdIns}(4,5)\text{P}_2$) greatly stimulates GTPase activity.¹⁴ The PH domain is not needed for self-assembly or GTPase activity; simply deleting it (delta-PH dynamin) maximally increases intrinsic GTPase activity.¹⁵ (iii) The GTPase effector domain (GED) controls dynamin–dynamin interactions and dynamin assembly into its basic tetrameric configuration, tetramers being subunits of the rings. About

* To whom correspondence should be addressed. A.M.: e-mail, Adam.McCluskey@newcastle.edu.au; phone, +61 249 216486; fax, +61 249 215472. P.J.R.: e-mail, phrobins@usyd.edu.au; phone, +61 296 872800; fax, +61 296 872120.

[†] The University of Newcastle.

[‡] Children's Medical Research Institute.

[§] The Scripps Research Institute.

^{||} Monash University.

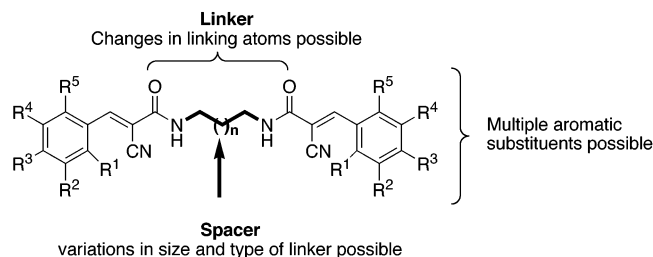
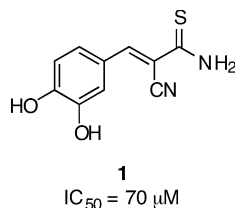


Figure 1. Library design for symmetrical dimeric analogues based on **2**.

28–32 tetramers cooperatively self-assemble as a single ring¹⁶ or as a helix around PtdIns(4,5)P₂-containing lipid mixtures.¹⁴ GED accounts for tetramer self-association by binding to the GTPase domain.¹⁷ GED acts like a GTPase activator protein to stimulate GTPase activity.¹⁸ (iv) The proline-rich domain (PRD) at dynamin's C-terminus interacts with many SH3 domain-containing proteins^{4,5} and calcineurin¹⁹ and is the site for *in vivo* dynamin phosphorylation.²⁰

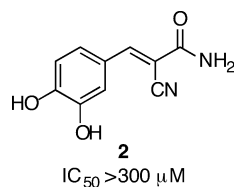
Our group recently discovered a series of long chain amine and ammonium salts that inhibit dynamin I GTPase activity.²¹ The most potent of these was myristoyl trimethyl ammonium bromide (MTMAB IC₅₀ = 3.2 ± 0.6 μM). These compounds inhibit dynamin by competing with lipid binding to the PH domain (unpublished observations). As part of these and ongoing studies in our laboratories we screened a small library of tyrphostins and discovered that **1** displayed good *in vitro* inhibition of dynamin I GTPase activity, while a large series of other tyrphostins were ineffective. Herein we report the design and synthesis of dynamin I inhibitors based on **1** and on the development of a structure activity profile.



Results and Discussion

Our initial library screening in the search for inhibitors of dynamin I GTPase activity identified (**1**) as a 70 μM potent lead.

Concerned about the known instability of **1**,²² we aimed to develop a series of new analogues, focusing initial synthetic efforts of the corresponding amido analogue 2-cyano-3-(3,4-dihydroxyphenyl)acrylamide (**2**) (Figure 1). Our primary targeted library synthesis was



designed to (a) determine the role of the aromatic substituents, both the type and positioning, and (b) determine the effect of additional substituents at the amide NH₂. With the 100 or so analogues synthesized,

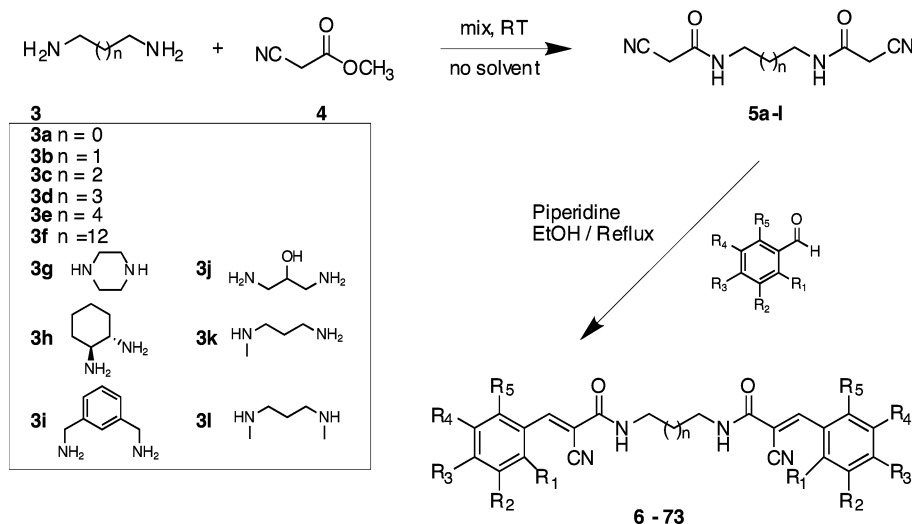
no dynamin I GTPase inhibition was noted (see Table S1, Supporting Information).²³

Somewhat surprised by the complete lack of inhibition, we reexamined the activity of **1** and noted that it increased as a function of time in solution. ES-MS experiments showed rapid decomposition of **1** in the presence of air and the appearance of two major product peaks (*m/z* = 366.95; 408.99; 444.97; 574.97 and 652.96), but not in the presence of DTT, a known quencher of disulfide formation. This is in keeping with reports by Wells²² that the decomposition of **1** is not solely a result of disulfide formation, but is more complex most likely involving oxidation of the catechol moieties. Thus the observed inhibitory action of **1** resides in a higher molecular weight analogue (see Supporting Information). Therefore, given the effect of DTT and synthetic ease we redirected our efforts to the synthesis of a second library of symmetrically substituted analogues of **2** (Figure 1). Related dimeric tyrphostins have been reported previously as potent inhibitors of EGF receptor tyrosine kinase activity.²⁴

Retrosynthetic analysis suggested that simple application of Knoevenagel chemistry involving substituted benzaldehydes and a series of appropriate α,ω-bisamines would rapidly afford the desired libraries (Scheme 1). To expedite the development of a SAR profile, we limited the choice of aromatic groups to thirteen commercially available benzaldehydes. In all cases good to excellent yields were obtained (see Experimental Section and Supporting Information).²¹

Utilization of this approach allowed the rapid generation of a number of discrete sublibraries, based upon the length of the alkane spacer arm with *n* = 1–4 and *n* = 10. Our library structure allowed variation in aromatic ring substitution facilitating the rapid examination of key features required such as spatial location/orientation of groups, the distances between aromatic rings, and the effect of electron donating and electron withdrawing groups, and in conjunction with biological screening, the development of a preliminary structure activity relationship. Initial biological screens for dynamin I GTPase activity were conducted at 100 μM. More promising analogues were then screened across a range of concentrations to determine their IC₅₀ values (Table 1). Of the 68 analogues synthesized only compounds **9–11**, **22–24**, **35–37**, **48–50**, and **61–63** showed noteworthy inhibition (operationally defined as having an IC₅₀ < 100 μM).

Within sublibrary 1 (*n* = 0), aromatic compounds containing no substitutions (**6**) or single –OH (**7**, **8**), –Cl (**12**, **13**), –OMe (**14**, **15**), or –COOH (**18**) showed no dynamin inhibition (Table 1). Introduction of a second oxygen-bearing substituent had a pronounced effect with the 3,4-di-OH (**9**) active (IC₅₀ = 5.1 ± 0.6 μM); however, monomethylation of the C3 –OH (**17**) and bis-methylation of C3 and C4 –OH (**16**) rendered the compounds inactive. Reintroduction of an oxygen-bearing substituent at C3 (or the equivalent C5-position) as an –OH resulted in low μM potency once more (**11**). Examination of the additional sublibraries (*n* = 1, 2, etc.) highlights a similar trend, i.e., there is a requirement for a minimum of two free –OH groups on each of the aromatic rings, and this trend is consistent through each of the subsequent sublibraries developed.

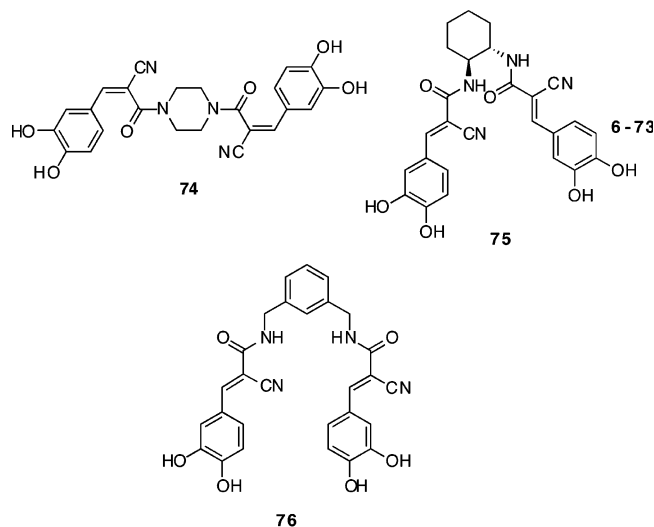
Scheme 1. Synthesis of a Dimeric Analogue of Library 2^a

^a Details of substituents R₁–R₅ and the alkane spacer n are given in Table 1.

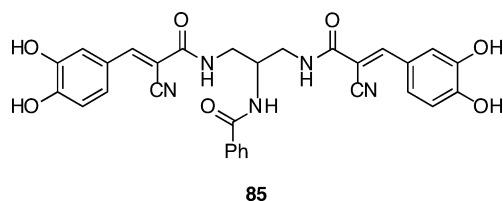
For example, the 3,4,5-trisubstituted aromatic compound **10** was equipotent with **23**. The corresponding compounds in each of the longer analogues **22–24**, **35–37**, **48–50**, and **61–63** all displayed some level of dynamin inhibiting activity, although these latter analogues are dropping off in potency.

Alkane spacer chain elongation had little effect on potency until $n > 3$. For example, chain extended analogues of **9** ($n = 0$), i.e., **22** ($n = 1$), **35** ($n = 2$), **48** ($n = 3$), **61** ($n = 4$), and **71** ($n = 10$) display IC₅₀ values of 5.1 ± 0.6 , 1.7 ± 0.2 , 3.2 ± 1.0 , 5.0 ± 1.4 , 26 ± 2 , and >100 μM , respectively. In contrast, while examining a raft of similar compounds against EGF receptor tyrosine kinase phosphorylation of the poly-GAT substrate, Gazit et al. observed that inhibition was independent of chain length.^{24–26}

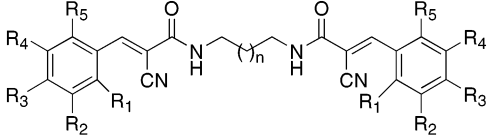
This contrasts with the effects of dimeric tyrosinases on tyrosine kinase potency, which resides in their extended configuration and thus allows them to fit the dimeric intermediate of the EGFR tyrosine kinases.^{24,25} Introduction of a more rigid linker such as piperazine (**74**) resulted in complete loss of activity (Table 2). Increasing the conformational flexibility (but still more rigid than the original straight chain linkers) with 1,2-bis-aminocyclohexane (**75**) and 1,3-bis-benzylamine (**76**), we note the return of sub 100 μM potencies of all these analogues, albeit markedly less potent than **9** (Table 2). We propose that the observed reduction in potency associated with **75** and **76** is due to increased conformational rigidity resulting in poor alignment of pivotal binding modes. Indeed, our synthetic efforts commencing with 1,3-bis-aminopropan-2-ol and application of similar chemistries to those described in Scheme 1 have shown that limited modifications at this point are permissible, and the introduction of an –OH with **82** is well tolerated (Table 2, Scheme 2). However the introduction of propyl or benzyl ether renders these analogues, **83** and **84**, inactive (Table 2).



Further synthetic modifications designed to probe requirements of the central linker were also explored. Installation of a benzoyl amide (**85**) via the azide and standard peptide coupling approaches²⁷ (Supporting Information) gave rise to the same outcome as that evidenced with ethers **83** and **84**, i.e., no inhibition of dynamin I GTPase.



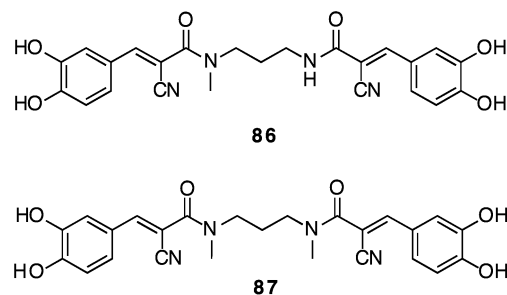
With analogues **83**, **84**, and **85** the lack of biological activity suggests that there is a finite binding pocket at this point and that only small groups are tolerated.

Table 1. Symmetrically Substituted Analogues of **2**: Effect of Aromatic Ring Modifications Analogues on Dynamin I GTPase Activity


compd	R ₁	R ₂	R ₃	R ₄	R ₅	n	IC ₅₀ (μM) ^a
6	H	H	H	H	H	0	—
7	H	OH	H	H	H	0	—
8	H	H	OH	H	H	0	—
9	H	H	OH	OH	H	0	5.1 ± 0.6
10	H	OH	OH	OH	H	0	1.7 ± 0.2
11	H	OMe	OH	OH	H	0	9.0 ± 3.0
12	Cl	H	H	H	H	0	—
13	H	H	H	Cl	H	0	—
14	H	OMe	H	H	H	0	—
15	H	H	OMe	H	H	0	—
16	H	H	OMe	OMe	H	0	—
17	H	H	OMe	OH	H	0	—
18	H	H	COOH	H	H	0	—
19	H	H	H	H	H	1	—
20	H	OH	H	H	H	1	—
21	H	H	OH	H	H	1	—
22	H	H	OH	OH	H	1	1.7 ± 0.2
23	H	OH	OH	OH	H	1	1.7 ± 0.2
24	H	OMe	OH	OH	H	1	5.0 ± 1.0
25	Cl	H	H	H	H	1	—
26	H	H	Cl	H	H	1	—
27	H	OMe	H	H	H	1	—
28	H	H	OMe	H	H	1	—
29	H	H	OMe	OMe	H	1	—
30	H	H	OMe	OH	H	1	—
31	H	H	COOH	H	H	1	—
32	H	H	H	H	H	2	—
33	H	OH	H	H	H	2	—
34	H	H	OH	H	H	2	—
35	H	H	OH	OH	H	2	3.2 ± 1.0
36	H	OH	OH	OH	H	2	2.1 ± 0.2
37	H	OMe	OH	OH	H	2	8.0 ± 0.2
38	Cl	H	H	H	H	2	—
39	H	H	H	Cl	H	2	—
40	H	OMe	H	H	H	2	—
41	H	H	OMe	H	H	2	—
42	H	H	OMe	OMe	H	2	—
43	H	H	OMe	OH	H	2	—
44	H	H	COOH	H	H	2	—
45	H	H	H	H	H	3	—
46	H	OH	H	H	H	3	—
47	H	H	OH	H	H	3	—
48	H	H	OH	OH	H	3	5.0 ± 1.4
49	H	OH	OH	OH	H	3	1.7 ± 0.4
50	H	OMe	OH	OH	H	3	8.0 ± 0.2
51	Cl	H	H	H	H	3	—
52	H	H	H	Cl	H	3	—
53	H	OMe	H	H	H	3	—
54	H	H	OMe	H	H	3	—
55	H	H	OMe	OMe	H	3	—
56	H	H	OMe	OH	H	3	—
57	H	H	COOH	H	H	3	—
58	H	H	H	H	H	4	—
59	H	OH	H	H	H	4	—
60	H	H	OH	H	H	4	—
61	H	H	OH	OH	H	4	26 ± 2
62	H	OH	OH	OH	H	4	6.0 ± 2.0
63	H	OMe	OH	OH	H	4	80 ± 4
64	Cl	H	H	H	H	4	—
65	H	H	H	Cl	H	4	—
66	H	OMe	H	H	H	4	—
67	H	H	OMe	H	H	4	—
68	H	H	OMe	OMe	H	4	—
69	H	H	OMe	OH	H	4	—
70	H	H	COOH	H	H	4	—
71	H	OH	OH	H	H	10	—
72	H	OH	OH	OH	H	10	—
73	H	OMe	OH	OH	H	10	—

^a IC₅₀ determinations conducted in triplicate; (—) > 100 μM.

Our SAR studies also indicate that N-methylation of one, **86**, or both, **87**, of the amide NH's of **9** is detrimental



to inhibition (Table 2). This suggests that the amide NH's also play an important role in binding to dynamin I, either by stabilization of the active conformation or by H-bonding within dynamin I GTPases active site (or both).

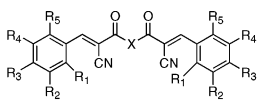
However, replacement of the amide linkage with the corresponding esters (Scheme 3) maintained a moderate level of inhibition, which again was dependent upon the spacer length (Table 3, analogues **90–93**). Presumably the reduction in inhibition is a result of the less favorable H-bonding characteristics of the ester “O” compared with the amide “NH”.²⁸

Having determined that the amide moiety was important for inhibitory activity, relative to the corresponding esters, and that methylation was detrimental, the final logical exploration in this preliminary study was delineation of the role of the pendant nitriles. This role was established via the synthesis of the corresponding cyano free analogues (Scheme 4). Synthesis commenced with 3,4-dihydroxycinnamic acid (**94**) and protection of the catechols as the corresponding acetates (**95**). Treatment with SOCl₂ in CHCl₃ with catalytic quantities of DMF afforded the acyl chloride disposed for addition of α,ω-bis-amines (**3a–e**) to yield the nitrile free acetates (**97a–e**), and acid cleavage (HCl) of the acetates gave the desired nitrile free analogues (**98–102**),²⁷ with varying spacer chain sizes as had been examined in our original sublibraries. Biological evaluation revealed the nitrile free analogues to be inactive.

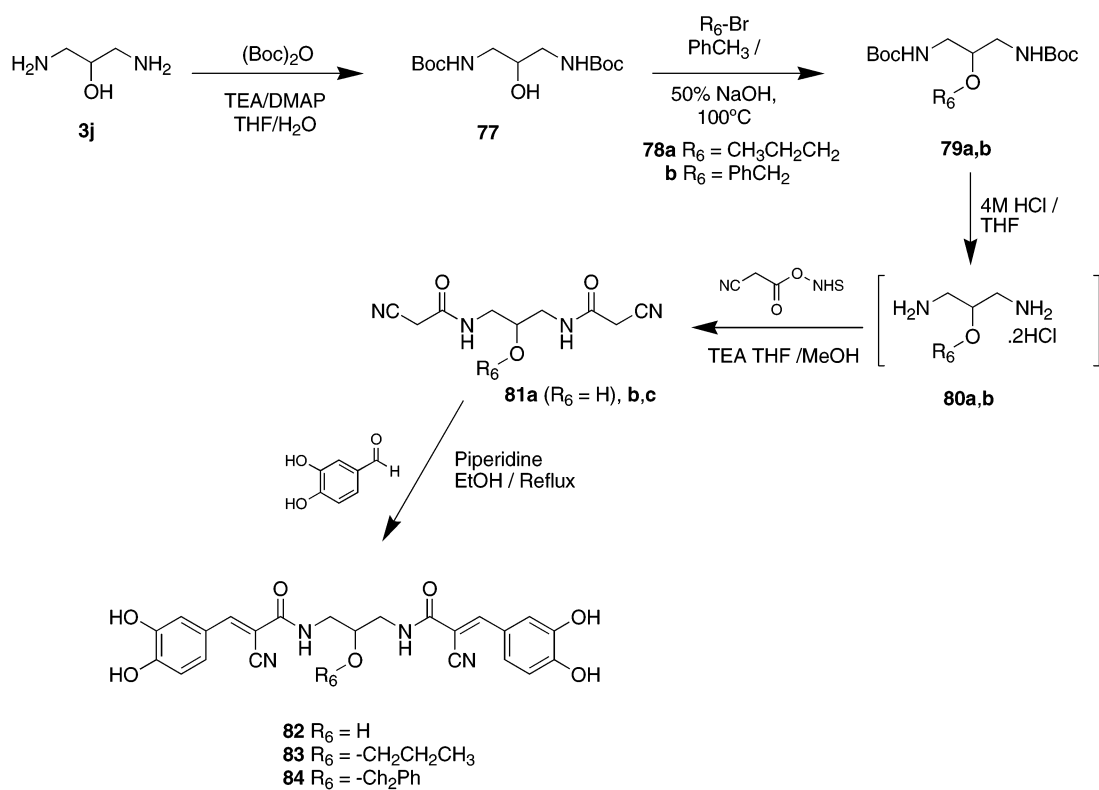
Conclusions

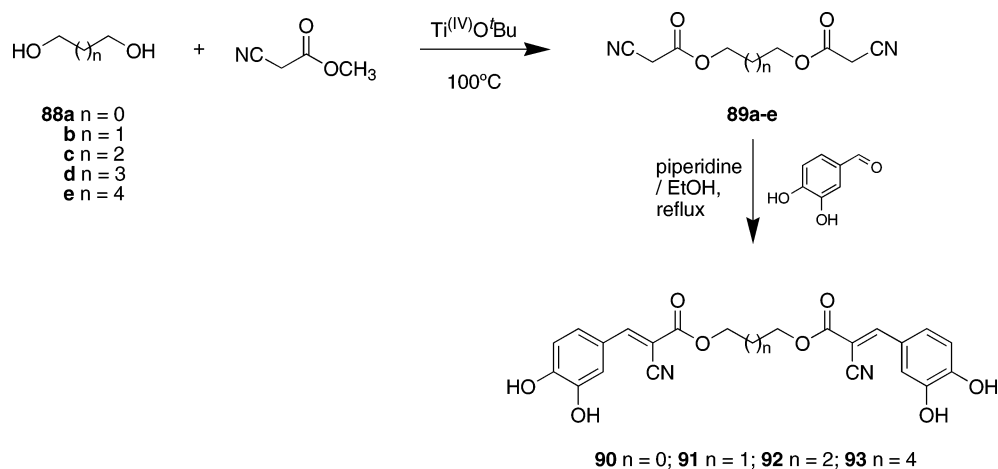
Herein we have reported the development of a preliminary structure–activity relationship of dimeric tyrophostins against the GTPase activity of the enzyme dynamin I. We believe that this represents a significant step forward in the development of specific dynamin GTPase inhibitors. From the data presented herein it is clear that inhibitory potency, for this class of compounds, requires a dimeric compound which contains two aromatic rings with these rings bearing 2 × –OH groups in the 3,4-positions; the presence of two free amide –NH's or an ester –O atom in the linker arm; and, also of considerable import is the presence of the –CN moieties.

As yet it is still unknown as to how these compounds are able to interact with dynamin, although we have preliminary evidence that these analogues are not GTP competitive (Robinson and McCluskey, unpublished observations). This study shows the first steps in developing a model for what is required for these compounds to interact with this enzyme.

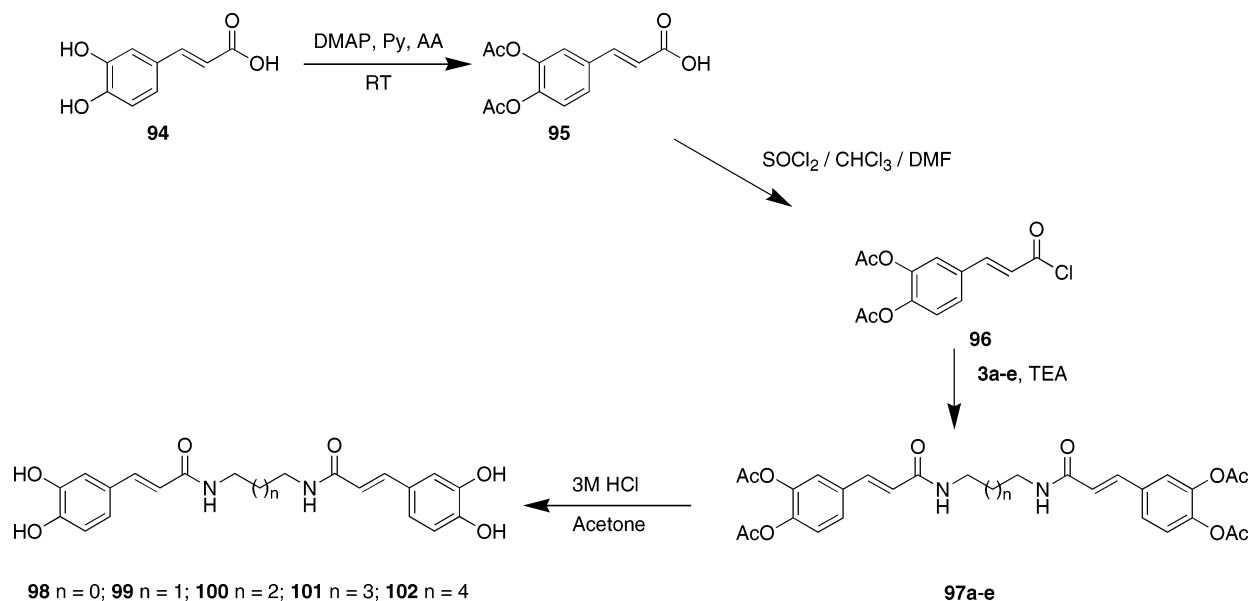
Table 2. Effect of Linker Modifications on Dynamin I GTPase Activity


Compound	R ¹	R ²	R ³	R ⁴	R ⁵	X	IC ₅₀ (μM) ^a
74	H	OH	OH	H	H		-
75	H	OH	OH	H	H		95±7
76	H	OH	OH	H	H		84±2
82	H	OH	OH	H	H		5.1±0.2
83	H	OH	OH	H	H		-
84	H	OH	OH	H	H		-
85	H	OH	OH	H	H		-
86	H	OH	OH	H	H		-
87	H	OH	OH	H	H		-

^a IC₅₀ determinations conducted in triplicate; (-) >100 μM.**Scheme 2.** Introduction of -OH (**82**), -OCH₂CH₂CH₃ (**83**), and -OCH₂Ph (**84**) into the Linker Units

Scheme 3. Synthesis of Ester Based Linker Analogues of **9**^a^a Cf. cyano acetate linkers of Scheme 1.**Table 3.** Effect of Introduction of Ester Linkers on Dynamin I GTPase Activity

Compound	R ¹	R ²	R ³	R ⁴	R ⁵	X	IC ₅₀ (μM) ^a
90	H	OH	OH	H	H		42±3
91	H	OH	OH	H	H		38±2
92	H	OH	OH	H	H		61±2
93	H	OH	OH	H	H		-

^a IC₅₀ determinations conducted in triplicate; (–) >100 μM.**Scheme 4.** Synthesis of Cyano Free Analogues of **9**

The most promising inhibitor compound in our study was 2-cyano-*N*-[3-[2-cyano-3-(3,4,5-trihydroxyphenyl)acryloylamino]ethyl]-3-(3,4,5-trihydroxyphenyl)acrylamide (**10**) ($IC_{50} = 1.7 \pm 0.2 \mu M$).²⁴ It will be of importance for subsequent studies to directly test the hypothesis that **22** may be an inhibitor of endocytosis in a cellular context.

Experimental Section

General. All starting materials were purchased from Aldrich Chemical Co. and Lancaster Synthesis. Solvents were bulk, and distilled from glass prior to use. ¹H and ¹³C spectra were recorded on a Bruker Advance AMX 300 MHz spectrometer at 300.13 and 75.48 MHz, respectively. Chemical shifts are relative to TMS as internal standard. All compounds returned satisfactory analyses. The Experimental Section details synthesis of previously unreported active analogues (**10**, **11**, **24**, **35**, **50**, **62**, **82**, **90**, **91**, and **92**) only; all other experimental detail is located in the Supporting Information.

Synthetic Methods. 2-Cyano-*N*-[3-[2-cyano-3-(3,4,5-trihydroxyphenyl)acryloylamino]ethyl]-3-(3,4,5-trihydroxyphenyl)acrylamide (**10**): synthesized as per **9** from 2-cyano-*N*-[3-(2-cyanoacetylaminomethyl)ethyl]acetamide (**5a**)²⁴ and 3,4,5-trihydroxybenzaldehyde; afforded an orange solid, 82%, mp >300 °C.

¹H NMR (DMSO): 8.29 (2H, t, *J* = 5.5 Hz), 7.79 (2H, s), 6.99 (4H, s), 3.32 (4H, br s). ¹³C NMR (DMSO): 162.2, 150.7, 145.9, 140.2, 121.3, 117.3, 110.0, 99.8, 39.4. Anal. (C₂₂H₁₈N₄O₈): C, H, N.

2-Cyano-*N*-[3-[2-cyano-3-(3,4-dihydroxy-4-methoxyphenyl)acryloylamino]ethyl]-3-(3,4-dihydroxy-5-methoxyphenyl)acrylamide (**11**): synthesized as per **9** from 2-cyano-*N*-[3-(2-cyanoacetylaminomethyl)ethyl]acetamide (**5a**)²⁴ and 3,4-dihydroxy-5-methoxybenzaldehyde; afforded an orange solid, 66%, mp 274 °C.

¹H NMR (DMSO): 8.34 (2H, t, *J* = 5.5 Hz), 7.93 (1H, s), 7.20 (2H, d, *J* = 1.92 Hz), 7.13 (2H, d, *J* = 1.92 Hz), 3.77 (6H, s), 3.35 (4H, br s). ¹³C NMR (DMSO): 161.9, 150.8, 148.0, 145.8, 139.9, 121.8, 117.2, 111.1, 107.2, 100.8. Anal. (C₂₄H₂₂N₄O₈·0.5H₂O): C, H, N.

2-Cyano-*N*-[3-[2-cyano-3-(3,4-dihydroxy-5-methoxyphenyl)acryloylamino]propyl]-3-(3,4-dihydroxy-5-methoxyphenyl)acrylamide (**24**): synthesized as per **9** from 2-cyano-*N*-[3-(2-cyanoacetylaminomethyl)propyl]acetamide (**5b**)²⁴ and 3,4-dihydroxy-4-methoxybenzaldehyde; afforded an orange solid, 42%, mp >300 °C.

¹H NMR (DMSO): 8.35 (2H, t, *J* = 5.4 Hz), 7.95 (2H, s), 7.21 (2H, d, *J* = 1.9 Hz), 7.12 (2H, d, *J* = 1.9 Hz), 3.21 (4H, q, *J* = 6.8 Hz), 1.71 (2H, quin, *J* = 6.8 Hz). ¹³C NMR (DMSO): 161.3, 150.6, 147.2, 145.3, 121.0, 117.6, 110.6, 107.6, 98.7, 38.4, 28.9. Anal. (C₂₅H₂₄N₄O₈·2H₂O): C, H, N.

2-Cyano-*N*-[3-[2-cyano-3-(3,4-dihydroxy-5-methoxyphenyl)acryloylamino]butyl]-3-(3,4-dihydroxy-5-methoxyphenyl)acrylamide (**37**): synthesized as per **9** from 2-cyano-*N*-[3-(2-cyanoacetylaminomethyl)butyl]acetamide (**5c**)²⁴ and 3,4-dihydroxy-5-methoxybenzaldehyde; afforded a yellow solid, 70%, mp >300 °C.

¹H NMR (DMSO): 8.09 (2H, t, *J* = 5.5 Hz), 7.86 (2H, s), 7.18 (2H, d, *J* = 1.9 Hz), 7.10 (2H, d, *J* = 1.9 Hz), 3.75 (6H, s), 3.19 (4H, br s), 1.48 (4H, br s).

¹³C NMR (DMSO): 161.7, 150.2, 148.7, 146.2, 120.3, 117.5, 109.5, 106.8, 98.8, 55.8, 39.3, 26.6.

Anal. (C₂₆H₂₆N₄O₈): C, H, N.

2-Cyano-*N*-[3-[2-cyano-3-(3,4-dihydroxy-5-methoxyphenyl)acryloylamino]pentyl]-3-(3,4-dihydroxy-5-methoxyphenyl)acrylamide (**50**): synthesized as per **9** from 2-cyano-*N*-[3-(2-cyanoacetylaminomethyl)pentyl]acetamide (**5d**)²⁴ and 3,4-dihydroxy-5-methoxybenzaldehyde; afforded a yellow solid, 81%, mp 256 °C.

¹H NMR (DMSO): 8.09 (2H, t, *J* = 5.5 Hz), 7.86 (2H, s), 7.18 (2H, d, *J* = 2 Hz), 7.10 (2H, d, *J* = 2 Hz), 3.75 (6H, s), 3.17 (4H, br s), 1.50 (4H, quin, *J* = 6.8 Hz), 1.28 (4H, quin, *J* = 6.9 Hz). ¹³C NMR (DMSO): 161.8, 150.5, 148.0, 146.2, 120.1,

117.8, 110.5, 107.8, 98.7, 55.7, 39.4, 28.6, 22.5. Anal. (C₂₇H₂₈N₄O₈): C, H, N.

2-Cyano-*N*-[3-[2-cyano-3-(3,4,5-trihydroxyphenyl)acryloylamino]hexyl]-3-(3,4,5-trihydroxyphenyl)acrylamide (**62**): synthesized as per **9** from 2-cyano-*N*-[3-(2-cyanoacetylaminomethyl)hexyl]acetamide (**5e**)²⁴ and 3,4,5-trihydroxybenzaldehyde; afforded a yellow solid, 67%, mp >300 °C.

¹H NMR (DMSO): 8.11 (2H, t, *J* = 5.5 Hz), 7.76 (2H, s), 6.98 (4H, s), 3.16 (4H, br s), 1.47 (4H, quin, *J* = 6.1 Hz), 1.28 (4H, br s). ¹³C NMR (DMSO): 161.8, 150.5, 146.0, 141.2, 120.7, 117.5, 109.9, 99.2, 39.7, 28.8, 26.0. Anal. (C₂₆H₂₆N₄O₈·2.5H₂O): C, H, N.

2-Cyano-*N*-[3-[2-cyano-3-(3,4-dihydroxy-5-methoxyphenyl)acryloylamino]hexyl]-3-(3,4-dihydroxy-5-methoxyphenyl)acrylamide (**63**): synthesized as per **9** from 2-cyano-*N*-[3-(2-cyanoacetylaminomethyl)hexyl]acetamide (**5e**)²⁴ and 3,4-dihydroxy-5-methoxybenzaldehyde; afforded a yellow solid, 86%, mp 243 °C.

¹H NMR (DMSO): 8.17 (2H, t, *J* = 5.5 Hz), 7.89 (2H, s), 7.19 (2H, d, *J* = 1.6 Hz), 7.13 (2H, d, *J* = 1.6 Hz), 3.77 (6H, s), 3.17 (4H, br s), 1.48 (4H, quin, *J* = 6.1 Hz), 1.29 (4H, br s). ¹³C NMR (DMSO): 161.8, 150.5, 146.1, 146.0, 141.3, 120.7, 117.5, 109.9, 99.1, 39.5, 28.6, 22.3. Anal. (C₂₈H₃₀N₄O₈·0.75H₂O): C, H, N.

2-Cyano-*N*-[3-[2-cyano-3-(3,4-dihydroxyphenyl)acryloylamino]-2-hydroxypropyl]-3-(3,4-dihydroxyphenyl)acrylamide (**82**): synthesized as per **9** from 2-cyano-*N*-[3-(2-cyanoacetylaminomethyl)-2-hydroxypropyl]acetamide (**5j**)²⁴ and 3,4-dihydroxybenzaldehyde (0.37 g, 2.7 mmol); afforded a yellow solid, 56%, mp 255 °C.

¹H NMR (DMSO): 7.9 (2H, t br), 7.86 (2H, s), 7.48 (2H, d, *J* = 2.0 Hz), 7.21 (2H, dd, *J* = 8.4 Hz, 2.3 Hz), 6.68 (2H, d, *J* = 8.4 Hz), 5.1 (OH, br), 3.72 (1H, quin, *J* = 5.8 Hz), 3.25 (4H, m). ¹³C NMR (DMSO): 162.5, 156.1, 150.5, 146.6, 127.2, 120.3, 118.1, 115.7, 113.7, 96.2, 68.0, 44.0, 22.2. Anal. (C₂₃H₂₀N₄O₇): C, H, N.

2-Cyano-3-(3,4-dihydroxyphenyl)acrylic acid 2-[2-cyano-3-(3,4-dihydroxyphenyl)acryloyloxy]ethyl ester (**90**): synthesized as per **9** from cyanoacetic acid 2-(2-cyanoacetoxy)ethyl ester (**89a**)²⁸ and 3,4-dihydroxybenzaldehyde; afforded a yellow solid, 73%, mp 232 °C.

¹H NMR (DMSO): 8.11 (2H, t br), 7.63 (2H, d, *J* = 2.1 Hz), 7.35 (2H, dd, *J* = 8.4 Hz, 2.2 Hz), 6.87 (2H, d, *J* = 8.3 Hz), 4.53 (4H, t br). ¹³C NMR (DMSO): 162.7, 155.1, 152.7, 145.8, 127.2, 122.6, 116.3, 116.2, 115.9, 95.7, 63.3. Anal. (C₂₂H₁₆N₄O₈): C, H, N.

2-Cyano-3-(3,4-dihydroxyphenyl)acrylic acid 2-[2-cyano-3-(3,4-dihydroxyphenyl)acryloyloxy]propyl ester (**91**): synthesized as per **9** from cyanoacetic acid 2-(2-cyanoacetoxy)propyl ester (**89b**)²⁸ and 3,4-dihydroxybenzaldehyde; afforded a yellow solid, 61%, mp 195 °C.

¹H NMR (DMSO): 8.08 (2H, t br), 7.61 (2H, d, *J* = 2.0 Hz), 7.35 (2H, dd, *J* = 8.4 Hz, 2.1 Hz), 6.82 (2H, d, *J* = 8.3 Hz), 4.32 (4H, t br), 1.63 (2H, quin br). ¹³C NMR (DMSO): 162.6, 155.3, 152.2, 145.6, 127.3, 122.6, 116.3, 116.2, 115.9, 95.4, 65.3, 24.2. Anal. (C₂₃H₁₈N₄O₈): C, H, N.

2-Cyano-3-(3,4-dihydroxyphenyl)acrylic acid 2-[2-cyano-3-(3,4-dihydroxyphenyl)acryloyloxy]butyl ester (**92**): synthesized as per **9** from cyanoacetic acid 2-(2-cyanoacetoxy)butyl ester (**89c**)²⁸ and 3,4-dihydroxybenzaldehyde; afforded a yellow solid, 48%, mp 252 °C.

¹H NMR (DMSO): 8.10 (2H, t br), 7.62 (2H, d, *J* = 2.0 Hz), 7.35 (2H, dd, *J* = 8.5 Hz, 2.0 Hz), 6.85 (2H, d, *J* = 8.5 Hz), 4.28 (4H, t br), 1.79 (4H, quin br). ¹³C NMR (DMSO): 162.8, 154.7, 152.9, 145.9, 127.2, 122.4, 116.4, 116.0, 115.9, 95.7, 65.2, 24.6. Anal. (C₂₄H₂₀N₄O₈): C, H, N.

GTPase Assay. Dynamin I was purified from sheep brain as previously described.⁶ Dynamin I GTPase activity was determined by hydrolysis of GTP by a method modified from that used previously.²⁹ Purified dynamin I (0.5 μg/well; 200 nM) was incubated in GTPase buffer (10 mM Tris, 10 mM NaCl, 2 mM Mg²⁺, 0.05% Tween 80, pH 7.4, 1 μg/mL leupeptin, and 0.1 mM PMSF) and GTP 0.3 mM in the presence of test compound for 12 min at 30 °C. The final assay volume was 40

μL . The assay was conducted in round-bottomed 96 well plates. The plates were prepared on ice, and the incubations of the plate were performed in a dry heating block with shaking (Eppendorf Thermomixer). Dynamin activity was measured as phospholipid stimulated with addition of 20 $\mu\text{g/mL}$ 1-phosphatidylserine (prepared by probe sonication). The reaction was terminated with 10 μL of 0.5 M EDTA pH 8.0, and the samples are then stable for several hours at room temperature. To each well was added 150 μL of Malachite green solution (Malachite green (50 mg), ammonium molybdate tetrahydrate (500 mg), 1 M HCl (50 mL): the solution was passed through 0.45 μm filters and stored in the dark for up to 2 months at room temperature).³⁰ Color developed for 5 min and was stable for as long as 2 h, and the sample absorbances in each plate were determined on a microplate reader at 650 nm. Phosphate release was quantified by comparison with a standard curve of sodium dihydrogen orthophosphate monohydrate (baked dry at 110 °C overnight) from 1 to 100 μM , which was run in each experiment.

Acknowledgment. We are grateful for financial support from the National Health & Medical Research Council (Australia), the Children's Medical Research Institute (CMRI), and the University of Newcastle (UN). T.H., L.R.O., and J.K.E. gratefully acknowledge scholarship support from UN & CMRI; UN; and UN & the Centre for Green Chemistry, respectively.

Supporting Information Available: Table of microanalysis data, experimental details, effects of analogues of **2** on dynamin I GTPase activity, and HPLC and MS study of degradation of **1**. This material is available free of charge via the Internet at <http://pubs.acs.org>.

References

- McLure, S. J.; Robinson, P. J. Dynamin, endocytosis and intracellular signaling. *Mol. Membr. Biol.* **1996**, *13*, 189–215.
- Cousin, M. A.; Robinson, P. J. Mechanisms of synaptic vesicle recycling illuminated by fluorescent dyes. *J. Neurochem.* **1999**, *73*, 2227–2239.
- Cousin, M. A.; Robinson, P. J. The dephosphins: Dephosphorylation by calcineurin triggers synaptic vesicle endocytosis. *Trends Neurosci.* **2001**, *24*, 659–665.
- Brodin, L.; Low, P.; Shupliakov, O. Sequential steps in clathrin-mediated synaptic vesicle endocytosis. *Curr. Opin. Neurobiol.* **2000**, *10*, 312–320.
- Hinshaw, J. E. Dynamin and its role in membrane fission. *Annu. Rev. Cell Dev. Biol.* **2000**, *16*, 483–519.
- Wang, L.-H.; Rothberg, K. G.; Anderson, R. G. Mis-assembly of clathrin lattices on endosomes reveals a regulatory switch for coated pit formation. *J. Cell Biol.* **1993**, *123*, 1107–1117.
- Gray, J. A.; Sheffler, D. J.; Bhatnagar, A.; Woods, J. A.; Hufeisen, S. J.; Benovic, J. L.; Roth, B. L. Cell-type specific effects of endocytosis inhibitors on 5-Hydroxytryptamine(2A) receptor desensitization and resensitization reveal an arrestin-, GRK2-, and GRK5-independent mode of regulation in human embryonic kidney 293 cells. *Mol. Pharmacol.* **2001**, *60*, 1020–1030.
- Davis, P. J.; Conwell, M. M.; Johnson, J. D. Reggianni, A.; Myers, M.; Murtaugh, M. P. Studies on the effects of dansylcadaverine and related compounds on receptor mediated endocytosis in cultured cells. *Diabetes Care* **1984**, *7* (Suppl. 1), 35–41.
- Larkin, J. M.; Brown, M. S.; Goldstein, J. L.; Anderson, R. G. Depletion of intracellular potassium arrests coated pit formation and receptor mediated endocytosis in fibroblasts. *Cell* **1983**, *83*, 273–285.
- Lindgren, C. A.; Emery, D. G.; Haydon, P. G. Intracellular Acidification Reversibly Reduces Endocytosis at the Neuromuscular Junction. *J. Neurosci.* **1997**, *17*, 3074–3084.
- Atwood, W. J. A combination of low-dose chlorpromazine and neutralizing antibodies inhibits the spread of JC virus (JCV) in a tissue culture model: Implications for prophylactic and therapeutic treatment of progressive multifocal leukoencephalopathy. *J. Neurovirol.* **2001**, *7*, 307–310.
- Marks, B.; Stowell, M. H.; Vallis, Y.; Mills, I. G.; Gibson, A.; Hopkins, C. R.; McMahon, H. T. GTPase activity of dynamin and resulting conformation change are essential for endocytosis. *Nature* **2001**, *410*, 231–235.
- Niemann, H. H.; Knetsch, M. L.; Scherer, A.; Manstein, D. J.; Kull, F. J. Crystal structure of a dynamin GTPase domain in both nucleotide-free and GDP-bound forms. *EMBO J.* **2001**, *20*, 5813–5821.
- Stowell, M. H.; Marks, B.; Wigge, P.; McMahon, H. T. Nucleotide-dependent conformational changes in dynamin: evidence for a mechanochemical molecular spring. *Nat. Cell Biol.* **1999**, *1*, 27–32.
- Scaife, R.; Venien-Bryan, C.; Margolis, R. L. Dual function C-terminal domain of dynamin-1: Modulation of self-assembly by interaction of the assembly site with SH3 domains. *Biochemistry* **1998**, *37*, 17673–17679.
- Hinshaw, J. E.; Schmid, S. L. Dynamin self-assembles into rings suggesting a mechanism for coated vesicle budding. *Nature* **1995**, *374*, 190–192.
- Muhlberg, A. B.; Warnock, D. E.; Schmid, S. L. Domain structure and intramolecular regulation of dynamin GTPase. *EMBO J.* **1997**, *16*, 6676–6683.
- Sever, S.; Muhlberg, A. B.; Schmid, S. L. Impairment of dynamin's GAP domain stimulates receptor-mediated endocytosis. *Nature* **1999**, *398*, 481–486.
- Lai, M. M.; Hong, J. J.; Ruggiero, A. M.; Burnett, P. E.; Slepnev, V. I.; De Camilli, P.; Snyder, S. H. The Calcineurin-Dynamin 1 Complex as a Calcium Sensor for Synaptic Vesicle Endocytosis. *J. Biol. Chem.* **1999**, *274*, 25963–25966.
- Powell, K. A.; Valova, V. A.; Malladi, C. S.; Jensen, O. N.; Larsen, M. R.; Robinson, P. J. Phosphorylation of Dynamin I on Ser-795 by Protein Kinase C Blocks Its Association with Phospholipids. *J. Biol. Chem.* **2000**, *275*, 11610–11617.
- Hill, T. A.; Odell, L. R.; Quan, A.; Ferguson, G.; Robinson, P. J.; McCluskey, A. Long Chain Amines and Long Chain Ammonium Salts As Novel Inhibitors of Dynamin GTPase Activity. *Bioorg. Med. Chem. Lett.* **2004**, *14*, 3275–3278.
- Wells, G.; Seaton, S.; Stevens, M. F. G.; Structural Studies on Bioactive Compounds. 32. Oxidation of Tyrophostin Protein Kinase Inhibitors with Hypervalent Iodine Reagents. *J. Med. Chem.* **2000**, *45*, 1550–1562.
- McCluskey, A.; Robinson, P. J.; Hill, T.; Scott, J. L.; Edwards, J. K. Green Chemistry Approaches to the Knoevenagel Condensation: Comparison of Ethanol, Water and Solvent Free (Dry Grind) Approaches. *Tetrahedron Lett.* **2002**, *43*, 3117–3120.
- Gazit, A.; Osherov, N.; Gilon, C.; Levitzki, A. Tyrophostins. 6. Dimeric Benzylidenemalononitrile Tyrophostins: Potent Inhibitors of EGF Receptor Tyrosine Kinase in Vitro. *J. Med. Chem.* **1996**, *39*, 4905–4911.
- Thompson, M.; Rewcastle, G. W.; Tercel, M.; Dobrusin, E. M.; Fry, D. W.; Kraker, A. J.; Denny, W. A. Tyrosine Kinase Inhibitors. 1. Structure–Activity Relationships for Inhibition of Epidermal Growth Factor Receptor Tyrosine Kinase Activity by 2,3-Dihydro-2-thioxo-1H-indole-3-alkanoic Acids and 2,2'-Dithiobis(1H-indole-3-alkanoic acids). *J. Med. Chem.* **1993**, *36*, 2459–2469.
- Maumder, A.; Gazit, A.; Levitski, A.; Nicklaus, M.; Yung, J.; Kohlhagen, G.; Pommier, Y. Effects of Tyrophostins, Protein Kinase Inhibitors, on Human Immunodeficiency Virus Type 1 Integrase. *Biochemistry* **1995**, *34*, 15111–15122.
- Benoist, E.; Loussouarn, A.; Remaud, P.; Chatal, J.-F.; Gestin, J.-F. Convenient and simplified approaches to N-monoprotected triaminopropane derivatives: Key intermediates for bifunctional chelating agent synthesis. *Synthesis* **1998**, 113–118.
- Namazi, H.; Assadpour, A.; Pourabbas, B.; Entezami, A. Polycondensation of bis(cyanoacetate) and 5a,10b-dihydrobenzofuro[2,3-b]benzofuran-2,9-dicarbaldehyde via Knoevenagel reaction: synthesis of donor-acceptor polymers containing shoulder-to-shoulder main chains. *J. Appl. Polym. Sci.* **2001**, *81*, 505–511.
- Tan, T. C.; Valova, V. A.; Malladi, C. S.; Graham, M. E.; Berven, L. A.; Jupp, O. J.; Hansra, G.; McClure, S.; Sarcevic, B.; Boadle, R.; Larsen, M.; Cousin, M. A.; Robinson, P. J. Cdk5 is essential for synaptic vesicle endocytosis. *Nat. Cell Biol.* **2003**, *5*, 701–710.
- Geladopoulos, T. P.; Sotiropoulos, T. G.; Evangelopoulos, A. E. A malachite green colorimetric assay for protein phosphatase activity. *Anal. Biochem.* **1991**, *192*, 112–116.

JM040208L